

# A quantum-mechanical heat engine operating in finite time. A model consisting of spin-1/2 systems as the working fluid

Eitan Geva and Ronnie Kosloff

*Department of Physical Chemistry and The Fritz Haber Research Center for Molecular Dynamics,  
The Hebrew University, Jerusalem 91904, Israel*

(Received 28 August 1991; accepted 21 October 1991)

The finite-time operation of a quantum-mechanical heat engine with a working fluid consisting of many noninteracting spin-1/2 systems is considered. The engine is driven by an external, time-dependent and nonrotating magnetic field. The cycle of operation consists of two adiabats and two isotherms. The analysis is based on the time derivatives of the first and second laws of thermodynamics. Explicit relations linking quantum observables to thermodynamic quantities are developed. The irreversible operation of this engine is studied in three cases: (1) The sudden limit, where the performance is found to be the same as that of the spin analog of the *Otto* cycle. This case provides the lower bound of efficiency. (2) The step-cycle operation scheme. Here, the optimization of power is carried out in the high-temperature limit (the "classical" limit). The results obtained are similar to those of Andresen *et al.* [Phys. Rev. A **15**, 2086 (1977)]. (3) The Curzon–Ahlborn operation scheme. The semigroup approach is used to model the dynamics. Then the power production is optimized. All the results obtained for Newtonian engines operating by the same scheme, such as the Curzon–Ahlborn efficiency, apply in the high-temperature limit. These results are obtained without the additional assumption of proximity to thermal equilibrium, implicitly implied by the use of Newtonian heat conduction in the original derivation. It seems that the results of the Curzon–Ahlborn analysis are always obtained in the high-temperature limit, irrespective of the details of the model. The performance beyond the classical limit is optimized numerically. The classical approximation is found to be valid for most of the spin-polarization range. The deviations from the classical limit depend heavily upon the specific nature of both the working fluid and the heat baths and exhibit great diversity and complexity.

## I. INTRODUCTION

The finite-time performance of engines has been intensively studied in recent years,<sup>1</sup> beginning with the model of the endoreversible heat engine presented by Curzon and Ahlborn.<sup>2</sup> The validity of the results obtained in these studies is limited in two respects.

(I) The working fluid and the heat baths are classical. This statement has a twofold meaning: First, the temperatures are high enough so that the equipartition theorem holds, thus making the energy a quasicontinuous quantity. Second, all the operators representing observables commute, so that interference effects are erased.

(II) The dynamics along the "thermal branches" is modeled by phenomenological heat transfer laws. Newtonian heat conduction,  $\dot{Q} = \kappa(T - T')$ , is by far the most popular choice (where  $\dot{Q}$  refers to a heat current,  $T$  to the absolute temperature, and  $\kappa$  to the heat conductivity; primed and unprimed quantities are related to the working fluid and the heat bath, respectively). Some attention has also been given to other heat transfer laws, mainly the linear law of irreversible thermodynamics,  $\dot{Q} = L(1/T' - 1/T)$ , and the Stefan–Boltzmann thermal radiation law,  $\dot{Q} = \alpha(T^4 - T'^4)$ .<sup>3</sup> Apart from being phenomenological, these laws are valid only near thermal equilibrium, thus disregarding the more complex relaxation dynamics far from equilibrium. Some general bounds on the performance of engines that are not limited with respect to the specific heat transfer law have

also been presented by Salamon *et al.*<sup>4</sup>

In a previous study, a laser was modeled as a quantum-mechanical heat engine, not limited in the above-mentioned sense.<sup>5</sup> The thermal relaxation dynamics was modeled by the semigroup formalism.<sup>6</sup> The power of this engine was optimized, and its efficiency at maximum power was found to converge to the Curzon–Ahlborn efficiency,<sup>2</sup>

$$\eta_{CA} = 1 - (T_c/T_h)^{1/2}, \quad (1.1)$$

in the classical limit. Furthermore, an intrinsic and pure quantum-mechanical source of irreversibility was found to reside in the mechanical coupling with the external world.

A new model of an endoreversible quantum-mechanical heat engine is presented in the present study. It belongs to the same class of engines for which the relaxation dynamics is modeled by the semigroup approach. It differs from the previous model in three respects.

I. The engine cycles mechanically, with an average net work production per cycle, rather than being operated continuously. It is therefore more suitable for comparison with generic models based on phenomenological heat transfer laws. The problem of simultaneous thermal contact with two heat baths is also avoided this way. On the other hand, a steady-state algebraic solution does not exist, and one must resort to the task of solving the differential equation involved.

II. The working fluid consists of spin-1/2 systems that, apart from being the simplest quantum-mechanical systems, have no real classical analog. (The working fluid in the previous

model was constructed from two coupled harmonic oscillators.)

III. The time dependence of the external driving field is controllable, rather than imposed.

Three main questions motivate this research.

1. Are the basic results of finite-time thermodynamics more general than their derivations suggest? For example, can the Curzon–Ahlborn efficiency be interpreted as a classical limit (i.e., a high-temperature limit), independent of how far from equilibrium the engine is operated?
2. Is most of finite-time thermodynamics in its present state merely the classical and near-equilibrium limit of a richer far-from-equilibrium quantum-mechanical finite-time thermodynamics? If so, how do quantum-mechanical engines approach this limit?
3. In what way does quantum mechanics *per se* affect the finite-time performance of engines?

We intend to explore these questions by analyzing models of quantum-mechanical heat engines and similar devices.

## II. THE ENGINE

### A. General setup

An engine is defined by its working fluid and cycle of operation. In each segment of the cycle the working fluid transforms one type of energy into another. The engine is carried through the cycle by an external driving force. For the spin-1/2 engine under discussion, these three constituents are as follows.

- I. A working fluid consisting of many noninteracting spin-1/2 systems.
- II. A cycle of the Carnot type, i.e., two isothermal branches connected by two adiabatic branches, none of which are assumed reversible. Throughout this paper “temperature” will refer to  $\beta$  rather than  $T$ , if not stated otherwise ( $\beta = 1/T$ , where  $T$  is the absolute temperature in energy units). Each of the spin-1/2 systems is thermally coupled to a heat bath of constant temperature  $\beta_h$  or  $\beta_c$  along the hot or cold isotherms, respectively ( $\beta_h < \beta_c$ ). In the present study  $\beta_h$  and  $\beta_c$  are assumed non-negative.
- III. An external time-dependent magnetic field. The field’s direction is chosen constant and along the positive  $z$  axis. The field’s magnitude, however, does change over time, but is not allowed to reach zero, where the two energy levels are degenerate.

### B. Definitions for energy, work, heat, and temperature

The Hamiltonian of the interaction between a magnetic moment  $\vec{M}$  and a magnetic field  $\vec{B}$  is given by  $\mathbf{H} = -\vec{M} \cdot \vec{B}$ . For a single-spin system  $\vec{M}$  is proportional to the spin angular momentum  $\vec{S}$ :  $\vec{M} = \gamma \vec{S}$ , where  $\gamma$  is the gyromagnetic constant. Since in our case  $\vec{B}$  is set along the positive  $z$  axis and is time dependent, the Hamiltonian is given by  $\mathbf{H}(t) = -\gamma S_z B_z(t)$ . We define  $\omega(t) = -\gamma B_z(t)$ .  $\omega$  is positive since  $\gamma$  is assumed negative (i.e.,  $\vec{S}$  and  $\vec{M}$  are in opposite directions). Throughout this paper we refer to  $\omega$  rather than  $B_z$  as “the field.” The Hamiltonian of an isolated single spin-1/2 in the presence of the field  $\omega(t)$  is then<sup>7</sup>

$$\mathbf{H}(t) = \omega(t) S_z. \quad (2.1)$$

It is important to realize that  $\omega$ , and therefore  $\mathbf{H}$ , are explicitly time dependent. We would also like to stress that the non-negative temperature and the positive magnetic field assumptions imply  $0 > S_z \geq -1/2$ , where  $S = \langle S_z \rangle$  (our units are such that  $\hbar = 1$ ). The internal energy of the spin is simply the expectation value of the Hamiltonian:  $E = \langle \mathbf{H} \rangle = \omega S$ .

The engine’s operation can be followed through the change in the observables of the working fluid. Using the Heisenberg picture for the rate of change of an operator one obtains

$$\dot{\mathbf{X}} = i[\mathbf{H}, \mathbf{X}] + \frac{\partial \mathbf{X}}{\partial t} + \mathcal{L}_D(\mathbf{X}), \quad (2.2)$$

where  $\mathcal{L}_D(\mathbf{X})$  is a dissipation term, originating from a thermal coupling of the spin to a heat bath. It will be given explicitly and discussed in Sec. V A.  $\mathbf{H}$  is the effective Hamiltonian of a spin coupled to a bath. In the weak-coupling limit it is substituted by the Hamiltonian of the thermally isolated spin given by Eq. (2.1). We implicitly refer to such a limit from now on.  $\partial \mathbf{X} / \partial t$  is the result of an explicit time dependence of  $\mathbf{X}$ . For obtaining the rate of change of energy we substitute  $\mathbf{X}$  by  $\mathbf{H}$  in Eq. (2.2), obtaining

$$\frac{dE}{dt} = \frac{d}{dt} \langle \mathbf{H} \rangle = \dot{\omega} \langle S_z \rangle + \omega \langle \mathcal{L}_D(S_z) \rangle = \dot{\omega} S + \omega \dot{S}. \quad (2.3)$$

This result is the time derivative of the first law of thermodynamics.<sup>5</sup> The instantaneous power is identified by  $P = \langle \partial \mathbf{H} / \partial t \rangle = \dot{\omega} S$ , and the instantaneous heat flow is identified by  $\dot{Q} = \langle \mathcal{L}_D(\mathbf{H}) \rangle = \omega \dot{S}$ .<sup>8</sup> The definitions for the work and heat inexact differentials then emerge naturally as

$$dW = S d\omega, \quad (2.4a)$$

$$dQ = \omega dS. \quad (2.4b)$$

The discussion above refers to a single spin-1/2. The energy, work, and heat are therefore given per single spin-1/2. This is justified in the absence of spin–spin interactions. In such a case, simply multiplying by the total number of spins will produce the same quantities for the working fluid as a whole.

The temperature  $\beta'$  of the working fluid is always well established for given  $S$  and  $\omega$  because, for a two-level system, it is always well defined by the following relation:

$$S = -\frac{1}{2} \tanh(\beta' \omega / 2). \quad (2.5)$$

### C. The adiabatic branch

In the absence of thermal coupling and therefore of a dissipation term in Eq. (2.2), the adiabatic dynamics is governed by a purely mechanical Heisenberg equation. Since  $S_z$  commutes with  $\mathbf{H}$  [Eq. (2.1)],  $S$  is a constant of the motion regardless of the time dependence of  $\omega$ . The von Neumann entropy is also constant along this branch since the evolution is unitary. [ $\sigma_{\text{vN}} = -\text{tr}(\hat{\rho} \ln \hat{\rho})$ , where  $\hat{\rho}$  is the density matrix. Here, as in the rest of the paper, we designate the entropy by  $\sigma$ , not to be confused with the polarization  $S = \langle S_z \rangle$ ]. The diagonal entropy ( $\sigma_d = -\sum_i \rho_{ii} \ln \rho_{ii}$ ) is

also a constant of the motion. This is because  $S_x$  and  $S_y$  do not contribute to the diagonal elements of  $\hat{\rho}$  when it is expanded in the Pauli matrices in the  $S_z$  representation. It is therefore convenient to assume  $\langle S_x \rangle = \langle S_y \rangle = 0$  from the beginning. Even if  $\langle S_x \rangle, \langle S_y \rangle \neq 0$  initially, these nonzero polarizations along the  $x$  or  $y$  axes will eventually be suppressed by the dissipation terms along the isothermal branches. This effective diagonality of  $\hat{\rho}$  (which also holds for the isothermal branches) implies that no interference effects will appear under the assumption of constant field direction imposed on the model. However, the working fluid is still nonclassical in the sense that the discrete nature of energy remains. Consequently, the adiabatic branches can be regarded as both instantaneous and reversible (i.e., entropy conserving), since  $S$  is a constant of the motion, irrespective of the time dependence of  $\omega$ .

Increasing  $\omega$  adiabatically enlarges the energy gap between the two energy levels. Since  $S$  is a constant of motion, the populations of the two levels do not change during this process. The working fluid's temperature  $T'$  therefore increases and its energy decreases. No heat exchange is involved, and increasing  $\omega$  therefore corresponds to the performance of work by the working fluid on the surroundings. The reverse process of adiabatically decreasing  $\omega$  corresponds to the performance of work by the surroundings on the working fluid. In both instances the total amount of work involved is given by  $W_{ad} = S(\omega_f - \omega_i)$ , where  $\omega_i$  and  $\omega_f$  are the initial and final values of  $\omega$ , respectively.

A basic difference exists between the spin-1/2 working fluid and a quantum ideal-gas working fluid consisting of many noninteracting particles contained in a box: when performing work on the surroundings, the temperature  $T'$  of the ideal gas decreases while that of the spin-1/2 increases. This is attributed to the following: All the particle's energy levels move uniformly when the volume changes, while the two energy levels of the spin-1/2 move in opposite directions when  $\omega$  changes. The sign of the spin's net energy change is determined by the change in the lower level (in the non-negative temperature case). The adiabatic energy-temperature relation of the spin therefore has a slope opposite to that of the particle in the box.

#### D. The isothermal branch

For the purpose of the present study it is sufficient to discuss only the isothermal branches for which the working fluid's initial and final temperatures are the same and equal to  $\beta'$  ( $\beta'$  is not necessarily equal to the bath temperature  $\beta$ ). Changing  $\omega$  isothermally from an initial value  $\omega_i$  to a final value  $\omega_f$  involves a total change of the energy  $E$  by

$$\Delta E_{iso} = -\frac{1}{2}\omega_f \tanh(\beta'\omega_f/2) + \frac{1}{2}\omega_i \tanh(\beta'\omega_i/2). \quad (2.6)$$

The specific allocation of  $\Delta E_{iso}$  to heat and work depends on the specific time dependence of  $\omega$  (the latter determines the net entropy production).

Increasing  $\omega$  isothermally corresponds to a decrease of the working fluid's energy by a release of both work and heat. It is also accompanied by a decrease in the working fluid's entropy (the opposite is true for the reverse process of

decreasing  $\omega$  isothermally). Two sources are responsible for the total energy change: one is the change in the energy gap between the energy levels (i.e., in  $\omega$ ), and the other is the change in the polarization (i.e., in  $S$ ).  $|\Delta E_{iso}|$  is therefore larger than  $|\Delta E_{ad}|$  for given  $\omega_i$  and  $\omega_f$ , since the latter involves the first source only.

The isothermal process described above differs from its ideal-gas analog:  $W$  and  $Q$  have the same sign in the former, and opposite signs in the latter. The reason for this is similar to that discussed in the context of the adiabatic branch.

#### E. The reversible cycle of the Carnot type

The reversible hot isotherm equation is given by

$$S = -\frac{1}{2} \tanh(\beta_h \omega / 2). \quad (2.7a)$$

The reversible cold isotherm equation is given by

$$S = -\frac{1}{2} \tanh(\beta_c \omega / 2). \quad (2.7b)$$

$\beta_h$  and  $\beta_c$  are the hot and cold bath temperatures, respectively.

The two adiabats connecting those two isotherms are given by

$$S = S_1, \quad S = S_2, \quad (2.8)$$

where  $S_1 < S_2$  by choice, and  $S_1, S_2 < 0$  since  $\beta_c$  and  $\beta_h$  are assumed non-negative.

It is most instructive to plot the cycle, whether reversible or not, in the  $(\omega, S)$  plane. The reversible cycle in this plane is shown in Fig. 1. Note that the reversible cycle is fully defined by the values of four parameters:  $\beta_h, \beta_c, S_1$ , and  $S_2$ . The efficiency of this cycle is maximal and is given by

$$\eta_{rev} = 1 - \beta_h / \beta_c. \quad (2.9)$$

#### III. THE ENGINE'S PERFORMANCE IN THE SUDDEN LIMIT

Operating the spin-1/2 engine in the sudden limit allows one to study the irreversible performance without going into the details of the relaxation mechanism (cf. Sec. V). Con-

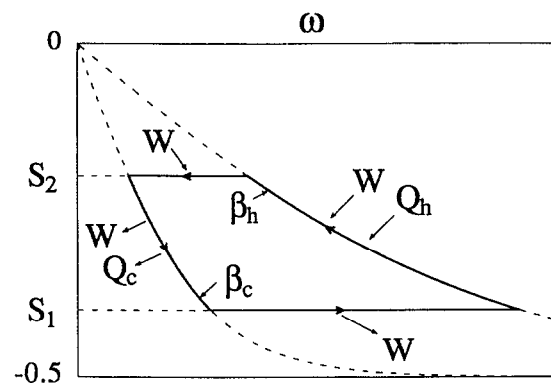


FIG. 1. The reversible Carnot cycle (solid line) in the  $(\omega, S)$  plane ( $\omega$  is the field and  $S$  the polarization). The cycle is composed of two reversible isotherms corresponding to the temperatures  $\beta_h$  and  $\beta_c$  ( $\beta_c > \beta_h$ ) and of two adiabats corresponding to the polarizations  $S_1$  and  $S_2$  ( $S_1 < S_2$ ;  $S_1, S_2 < 0$ ). Positive net work production is obtained by going anticlockwise. The directions of work and heat flows along each branch are indicated.

nections are then established between the quantum-mechanical engine and similar classical engines. These links will guide us in what follows.

The reversible cycle corresponds to the limit  $\dot{\omega} \rightarrow 0$ , where  $\omega$  changes very slowly on the time scale of the polarization thermal relaxation, and therefore maximizes efficiency. The sudden limit corresponds to the opposite limit of  $\dot{\omega} \rightarrow \infty$ , where  $\omega$  changes very fast on the time scale of the polarization thermal relaxation, and it therefore leads to minimal efficiency. These two extremes delimit the range of efficiencies that can be obtained from all the irreversible cycles going through the same four vertices.

The sudden limit cycle ( $1 \rightarrow 1' \rightarrow 2 \rightarrow 3 \rightarrow 3' \rightarrow 4 \rightarrow 1$ ) is shown in Fig. 2, where the corresponding reversible cycle for the same temperatures  $\beta_c, \beta_h$  and polarizations  $S_1, S_2$  is also plotted ( $1 \rightarrow 2 \rightarrow 3 \rightarrow 4 \rightarrow 1$ ). The cycles share the same adiabatic branches since  $S$  is constant along them regardless of  $\omega(t)$ . Both sudden limit isothermal branches are composed of two sub-branches: a very fast (i.e., sudden) change of  $\omega$  during which the polarization remains constant ( $1 \rightarrow 1', 3 \rightarrow 3'$ ), followed by a relaxation of the polarization at constant  $\omega$  until thermal equilibrium is attained ( $1' \rightarrow 2, 3' \rightarrow 4$ ). The former sub-branches are adiabatic since they do not involve heat transfer. A finite-temperature difference between the working fluid and the bath is therefore created. This temperature difference induces the thermal relaxation in the latter sub-branches. The sudden limit efficiency, which is the lower bound on efficiency for given  $\beta_c, \beta_h, S_1$ , and  $S_2$ , is obtained by applying Eq. (2.4) and is given by

$$\eta_{\text{sud}} = 1 - \frac{\omega_4}{\omega_2} = 1 - \frac{\beta_h}{\beta_c} \frac{\omega_1}{\omega_2} = 1 - \frac{\beta_h \tanh^{-1}(2S_1)}{\beta_c \tanh^{-1}(2S_2)} \quad (3.1)$$

$\eta_{\text{sud}}$  is smaller than  $\eta_{\text{rev}}$  since  $|S_1| > |S_2|$  and greater than zero since  $\omega_4 < \omega_2$  must hold if the working fluid is to perform work on the surroundings (see Fig. 2).

The universal entropy production per cycle is given by  $\Delta\sigma_{\text{cycle}} = -(\beta_h Q_h + \beta_c Q_c)$ , where  $Q_c$  and  $Q_h$  are the amounts of heat delivered between the working fluid and the

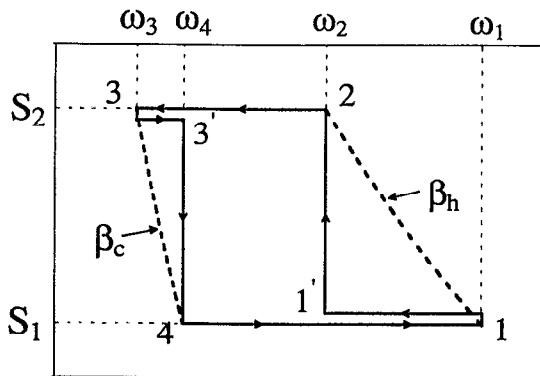


FIG. 2. The cycle at the sudden limit (thick solid line) in the  $(\omega, S)$  plane. The sub-branches  $1 \rightarrow 1'$  and  $1' \rightarrow 1$  converge in reality and were separated because of the limitations of the plot. The same holds for the sub-branches  $3 \rightarrow 3'$  and  $3' \rightarrow 3$ . The reversible isotherms at temperatures  $\beta_h$  and  $\beta_c$  are also shown (thick dashed lines).

cold and hot baths, respectively. In the sudden limit one can obtain, using Eq. (2.4),

$$\Delta\sigma_{\text{cycle}}^{\text{sud}} = 2(S_2 - S_1) [\tanh^{-1}(2S_2) - \tanh^{-1}(2S_1)], \quad (3.2)$$

which is the upper bound of  $\Delta\sigma_{\text{cycle}}$  for given  $S_1$  and  $S_2$  (the lower bound is obtained for the reversible cycle:  $\Delta\sigma_{\text{cycle}}^{\text{rev}} = 0$ ).

Since the sub-branches  $1 \rightarrow 1', 3 \rightarrow 3'$  merge with the adiabats, the performance of the cycle  $1 \rightarrow 1' \rightarrow 2 \rightarrow 3 \rightarrow 3' \rightarrow 4 \rightarrow 1$  is the same as that of the cycle  $1' \rightarrow 2 \rightarrow 3' \rightarrow 4 \rightarrow 1'$ . The latter is the spin-1/2 analog of the *Otto* cycle, usually discussed in terms of volume work performed by a working fluid running through a cycle composed of two adiabats and two isochores.<sup>9</sup> The efficiency of an *Otto* cycle with an ideal gas as the working fluid is given by  $\eta_{\text{Otto}}^g = 1 - (V_b/V_a)^{\gamma-1}$ , where  $V_a$  and  $V_b$  are the constant volumes along the two isochores ( $V_a > V_b$ ). A comparison of the ideal-gas adiabat equation:  $T_a/T_b = (V_a/V_b)^{1-\gamma}$ , to that of the spin-1/2 system:  $T_a/T_b = \omega_a/\omega_b$ , leads by way of analogy to the following *Otto* cycle efficiency for the spin-1/2 engine:  $\eta_{\text{spin}}^{\text{Otto}} = 1 - \omega_4/\omega_2$ . This is identical, as expected, to  $\eta_{\text{sud}}$  [Eq. (3.1)]. The entropy production given in Eq. (3.2) for the sudden limit cycle is also identical to that of the *Otto* cycle operating between the same polarizations and for the same reason.

#### IV. THE STEP CYCLE

All the points along the reversible isotherm correspond to equilibrium states, while only the two edges of the sudden limit isotherm correspond to equilibrium states. The step isotherm lies between these two extremes: a finite number,  $N + 1$ , of equilibrium states (including the edges) are distributed along it. A cycle composed of such step branches, with an ideal gas as the working fluid, was one of the first models analyzed in finite-time thermodynamics by Andresen *et al.*<sup>10</sup> Each step going from the  $n$ th equilibrium state to the  $(n + 1)$ th equilibrium state involves two substeps: first a sudden change of  $\omega$  from  $\omega_n$  to  $\omega_{n+1}$ , during which  $S$  remains constant and equal to

$$S_n = -\frac{1}{2} \tanh(\beta\omega_n/2),$$

followed by thermal relaxation of  $S$  to its new equilibrium value

$$S_{n+1} = -\frac{1}{2} \tanh(\beta\omega_{n+1}/2)$$

( $\beta$  is the temperature of the heat bath).

Let  $\omega_0, \omega_1, \omega_2, \dots, \omega_N$  be the values of the field at the equilibrium points along the step isotherm. Such a step isotherm is shown in Fig. 3.  $\omega_0$  and  $\omega_N$ —the values at the edges—are considered as constraints, while  $\omega_1, \omega_2, \dots, \omega_{N-1}$  are the variables whose value at the point of maximum work production we seek. The total work along the isotherm is given by

$$W(\omega_1, \omega_2, \dots, \omega_{N-1}) = \int_{\omega_0}^{\omega_N} S d\omega = \sum_{n=0}^{N-1} S_n (\omega_{n+1} - \omega_n). \quad (4.1)$$

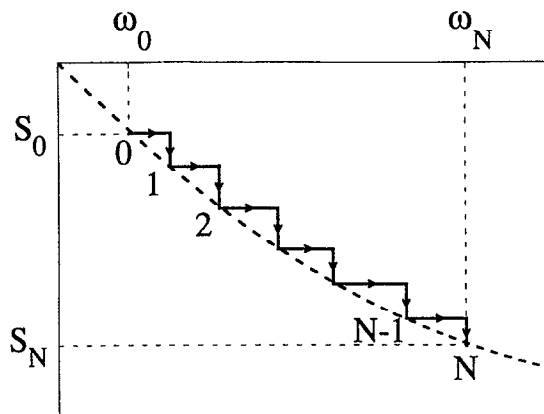


FIG. 3. The step isotherm for the case of increasing the field in  $N$  steps from  $\omega_0$  to  $\omega_N$  (thick solid line). The corresponding reversible isotherm is also shown (thick dashed line).

The values of  $\omega_1, \dots, \omega_{N-1}$  at the extremum of  $W$  can be obtained by solving the following set of  $N-1$  coupled and nonlinear equations:

$$\frac{\partial W}{\partial \omega_m} = \frac{1}{2} \left[ \tanh(\beta \omega_m / 2) - \tanh(\beta \omega_{m-1} / 2) - \frac{\beta \omega_{m+1} / 2 - \beta \omega_m / 2}{\cosh^2(\beta \omega_m / 2)} \right] = 0, \quad (4.2)$$

where  $m = 1, 2, \dots, N-1$ . Unlike their ideal-gas analog, these equations cannot be solved analytically. However, since using the equation of state of an ideal gas is equivalent to taking the classical limit, the same procedure is adopted for the spin-1/2 fluid. Now, spin-1/2 systems do not have a real classical limit. They do have a high-temperature limit which is usually referred to as "classical" in a loose manner. Taking this limit ( $\beta \omega_n \ll 1$  for every  $n$ ), Eq. (4.2) simplifies to

$$\omega_{m+1} - \omega_m = \omega_m - \omega_{m-1}, \quad (4.3)$$

which is readily solved by

$$\omega_m = \omega_0 + m \Delta \omega, \quad (4.4)$$

where  $\Delta \omega = (\omega_N - \omega_0) / N$ . Substituting these values back into Eq. (4.1) and taking the classical limit gives  $W^*$ , the extremal value of  $W$  at this limit:

$$W^* = -\frac{1}{8} \beta (\omega_N - \omega_0) (\omega_N + \omega_0 - \Delta \omega). \quad (4.5)$$

All the results in the remainder of this section refer to the classical limit. Note that  $\Delta \omega \rightarrow 0$  as  $N \rightarrow \infty$ , so that

$$W^* \rightarrow -\frac{1}{8} \beta (\omega_N^2 - \omega_0^2),$$

which is indeed the reversible work performed along the isotherm.

A step cycle composed of two step isotherms corresponding to heat baths at temperatures  $\beta_h$  and  $\beta_c$  ( $\beta_h < \beta_c$ ) and two adiabats  $S = S_1$  and  $S = S_2$  connecting them ( $S_1 < S_2$ ) is shown in Fig. 4. Let  $N_c$  and  $N_h$  be the numbers of steps along the cold and hot step isotherms, respectively. We would like to find the values of  $N_c$  and  $N_h$  at the point of maximum work production per cycle, under the constraint  $N_c + N_h = N$  where  $N$ , the total number of steps at both isotherms, is considered constant.

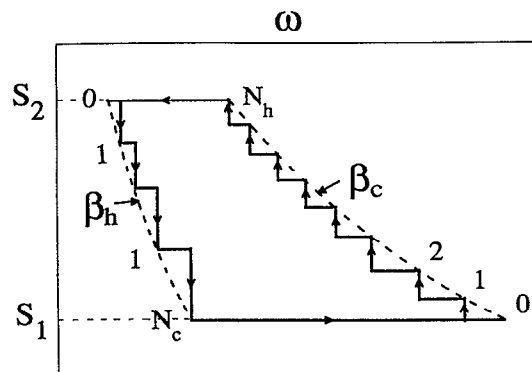


FIG. 4. The step cycle composed of two step isotherms at temperatures  $\beta_h$  and  $\beta_c$  and two adiabats at the polarizations  $S_1$  and  $S_2$  (solid line). The corresponding reversible isotherms at temperatures  $\beta_h$  and  $\beta_c$  are also shown (thick dashed lines).

Applying Eq. (4.5) to both isotherms, we obtain the following Lagrangian:

$$L(N_c, N_h) = -\frac{1}{8} \beta_h (\omega_2 - \omega_1) \left( \omega_2 + \omega_1 - \frac{\omega_2 - \omega_1}{N_h} \right) - \frac{1}{8} \beta_c (\omega_4 - \omega_3) \left( \omega_4 + \omega_3 - \frac{\omega_4 - \omega_3}{N_c} \right) - \lambda (N - N_c - N_h), \quad (4.6)$$

where  $\lambda$  is a Lagrange multiplier. The values of  $N_c$  and  $N_h$  at the extremum are obtained from the solution of the following equations:

$$\frac{\partial L}{\partial N_h} = \frac{-\beta_h (\omega_2 - \omega_1)^2}{N_h^2} + \lambda = -\frac{8}{\beta_h N_h^2} (S_2 - S_1)^2 + \lambda = 0, \quad (4.7a)$$

$$\frac{\partial L}{\partial N_c} = \frac{-\beta_c (\omega_4 - \omega_3)^2}{N_c^2} + \lambda = -\frac{8}{\beta_c N_c^2} (S_2 - S_1)^2 + \lambda = 0. \quad (4.7b)$$

The solution implies that the point of maximum work production is achieved when the total number of steps,  $N$ , is distributed in such a way that

$$\frac{N_c}{N_h} = \left( \frac{\beta_h}{\beta_c} \right)^{1/2}. \quad (4.8)$$

Andresen *et al.*<sup>10</sup> obtained the same result for the ideal-gas step cycle as a second-order approximation in  $1/N_c$  and  $1/N_h$ , i.e., approaching the reversible operation scheme. For the spin-1/2 step cycle Eq. (4.8) is valid at the classical limit which does not involve any assumption concerning closeness to reversible operation.

The step-cycle scheme does not involve time explicitly. The relaxation period at each step is infinitely long, in principle, since equilibrium is only reached asymptotically. However, a characteristic finite relaxation time can be defined, and in this sense the total number of steps  $N$  may be regarded

as a substitute for the total time period of the cycle. An optimization of the total work per cycle under the constraint of constant  $N$  is therefore equivalent to the optimization of power. If so, the term  $(\beta_h/\beta_c)^{1/2}$  appears again in the context of maximum power. [It first appeared in the Curzon-Ahlborn efficiency at maximum power, Eq. (1.1).] The in-

teresting question of whether this is a pure incident or not will be discussed in the next section. It becomes even more interesting if we recall that the step cycle is, in fact, very different from the Curzon-Ahlborn cycle. For example, its efficiency at maximum power is not at all that given by Eq. (1.1). Instead, it is given by

$$\eta_{\max}^{\text{step}} = \frac{(S_1 + S_2)(1 - \beta_h/\beta_c) + [(S_2 - S_1)/N][1 - (\beta_h/\beta_c)^{1/2}]}{(S_1 + S_2) + [(S_2 - S_1)/N][1 + (\beta_h/\beta_c)^{1/2}]} \quad (4.9)$$

The effectiveness of the step cycle at maximum power is given by

$$\frac{W_{\max}^{\text{step}}}{W_{\text{rev}}} = 1 - \frac{1}{N} \frac{1}{1 - (\beta_h/\beta_c)^{1/2}} \times \frac{\tanh^{-1}(2S_1) - \tanh^{-1}(2S_2)}{\tanh^{-1}(2S_1) + \tanh^{-1}(2S_2)} \quad (4.10)$$

As  $N \rightarrow \infty$  the effectiveness approaches 1 from below as  $1/N$ . The entropy production per cycle is given at maximum power by

$$\Delta\sigma_{\text{cycle}}^{\text{step}} = \frac{2(S_2 - S_1)^2}{N} [(\beta_c/\beta_h)^{1/2} - (\beta_h/\beta_c)^{1/2}]. \quad (4.11)$$

## V. THE CYCLE OF THE CURZON-AHLBORN TYPE, BASED UPON THE SEMIGROUP FORMALISM

### A. The equation of motion in the semigroup formalism

In order to discuss the engine's performance we must solve the equation of motion that determines the time evolution of  $S$ . This should be done for the case of a spin-1/2 system coupled mechanically to the given  $\omega(t)$  and thermally to a heat bath of temperature  $\beta$ . The inclusion of thermal coupling raises the problem of non-Hamiltonian evolution. No explicit equation of motion that can claim universal validity can be written in such a case. The semigroup approach<sup>6</sup> provides one pragmatic way out of this dilemma. The general scheme is as follows.

(1) Assume Hamiltonian evolution of the extended system consisting of the system and the bath.

(2) Mask the Hilbert space of the bath by performing a partial trace and obtain the reduced dynamical map of the system:  $\Lambda(t)$ .

(3) Impose axiomatically the semigroup condition on these reduced dynamical maps. The main assumption associated with this condition is Markovity in the following sense:  $\Lambda(t_1 + t_2) = \Lambda(t_1)\Lambda(t_2)$ . It is then shown that all the possible dynamical semigroup maps are generated by an equation of motion of a general form which, when given in the Heisenberg picture, reads as follows:

$$\dot{\mathbf{X}} = i[\mathbf{H}, \mathbf{X}] + \frac{\partial \mathbf{X}}{\partial t} + \mathcal{L}_D(\mathbf{X}),$$

$$\mathcal{L}_D(\mathbf{X}) = \sum_{\alpha} \gamma_{\alpha} (\mathbf{V}_{\alpha}^{\dagger} [\mathbf{X}, \mathbf{V}_{\alpha}] + [\mathbf{V}_{\alpha}^{\dagger}, \mathbf{X}] \mathbf{V}_{\alpha}). \quad (5.1)$$

$\mathbf{X}$ ,  $\mathbf{V}_{\alpha}$ ,  $\mathbf{V}_{\alpha}^{\dagger}$ , and  $\mathbf{H}$  are operators in the Hilbert space of the system.  $\mathbf{H}$  is the effective Hamiltonian of the system when coupled to the bath and may be substituted by the Hamiltonian of the isolated system in the weak-coupling limit.  $\mathbf{V}_{\alpha}$  and  $\mathbf{V}_{\alpha}^{\dagger}$  are Hermitian conjugates and like  $\mathbf{H}$  are not given by the theory.  $\gamma_{\alpha}$  are phenomenological positive coefficients. Equations of the form of Eq. (5.1) were obtained for the asymptotic time evolution, in the weak-coupling limit, in the singular bath limit, and in several specific cases where the reduction scheme can be performed.<sup>11</sup>

In our case "the bath" is a heat bath of constant temperature  $\beta$  and "the system" is the working fluid.  $\mathbf{V}_{\alpha}$  are chosen to be the spin creation and annihilation operators:  $\mathbf{S}_{+} = \mathbf{S}_x + i\mathbf{S}_y$  and  $\mathbf{S}_{-} = \mathbf{S}_x - i\mathbf{S}_y$ , and  $\mathbf{H} = \omega\mathbf{S}_z$ . Equation (5.1) is transformed by this setting into

$$\dot{\mathbf{X}} = i\omega[\mathbf{S}_z, \mathbf{X}] + \frac{\partial \mathbf{X}}{\partial t} + \gamma_{+} (\mathbf{S}_{-} [\mathbf{X}, \mathbf{S}_{+}] + [\mathbf{S}_{-}, \mathbf{X}] \mathbf{S}_{+}) + \gamma_{-} (\mathbf{S}_{+} [\mathbf{X}, \mathbf{S}_{-}] + [\mathbf{S}_{+}, \mathbf{X}] \mathbf{S}_{-}). \quad (5.2)$$

Substituting  $\mathbf{X} = \mathbf{S}_z$  in Eq. (5.2) and taking the expectation value results in the polarization relaxation equation,

$$\dot{S} = \langle \mathcal{L}_D(\mathbf{S}_z) \rangle = -2(\gamma_{+} + \gamma_{-})S - (\gamma_{-} - \gamma_{+}). \quad (5.3)$$

If  $\omega$  is constant,  $\gamma_{+}$  and  $\gamma_{-}$  are also constants, and the solution of Eq. (5.3) is given by

$$S(t) = S_{\text{eq}} + [S(0) - S_{\text{eq}}] e^{-2(\gamma_{+} + \gamma_{-})t}, \quad (5.4)$$

where

$$S_{\text{eq}} = -\frac{1}{2} \frac{\gamma_{-} - \gamma_{+}}{\gamma_{-} + \gamma_{+}}$$

is the asymptotic value of  $S$ . This asymptotic polarization must correspond to the value at thermal equilibrium:

$$S_{\text{eq}} = -\frac{1}{2} \tanh(\beta\omega/2).$$

Comparison of these two expressions for  $S_{\text{eq}}$  yields the detailed balance relation:

$$\gamma_{-}/\gamma_{+} = e^{\beta\omega}. \quad (5.5)$$

$\gamma_{+}$  and  $\gamma_{-}$  must satisfy Eq. (5.5) in order to bring the system to the correct equilibrium state asymptotically. A second relation is needed in order to determine the specific route to the asymptotic target, i.e., the individual values of  $\gamma_{+}$  and  $\gamma_{-}$ . The dynamical information associated with such a relation must be based upon a much more detailed

and therefore restrictive model of the bath and of the way it couples to the spin system.

Now, if  $\omega$  is explicitly time dependent, as it is in the problem we study, the asymptotic target, i.e.,

$$S_{\text{eq}} = -\frac{1}{2} \tanh[\beta\omega(t)/2],$$

is also time dependent. In other words, we control  $S$  by changing  $\omega$  in much the same way we would guide a horse by pulling a carrot. This implies an instantaneous detailed balance relation that must be satisfied by  $\gamma_+$  and  $\gamma_-$  (now also explicitly time dependent):

$$\gamma_- / \gamma_+ = e^{\beta\omega(t)}. \quad (5.6)$$

In order to proceed, the specific time dependence of  $\gamma_+$  and  $\gamma_-$  must be set. Since  $\gamma_+$  and  $\gamma_-$  are constant for constant  $\omega$ , it is natural to suppose that their time dependence stems solely from that of  $\omega$ . We assume the simplest possibility complying with Eq. (5.6), that is,

$$\gamma_+ = ae^{q\beta\omega}, \quad \gamma_- = ae^{(1+q)\beta\omega}, \quad (5.7)$$

where  $q$  and  $a$  are constant parameters to be obtained from a more detailed model of the bath. Since  $\gamma_+, \gamma_- > 0$ ,  $a > 0$  must hold. Since for  $\beta \rightarrow \infty$ ,  $\gamma_+ \rightarrow 0$  and  $\gamma_- \rightarrow \infty$  so that  $\gamma_- / \gamma_+ = e^{\beta\omega}$ ,  $0 > q > -1$  must hold. Substituting Eq. (5.7) into Eq. (5.3), one obtains

$$\dot{S} = -ae^{q\beta\omega} [2(1 + e^{\beta\omega})S + (e^{\beta\omega} - 1)]. \quad (5.8)$$

In Eq. (5.8),  $\omega(t)$  is imposed and  $S(t)$  is sought. Since  $\omega(t)$  is assumed monotonic,  $t(\omega)$  is a single-valued function, so that  $S$  can be written as a function of  $\omega$ ,  $S(\omega)$ , rather than  $S(t)$  [ $S(\omega)$  is really the irreversible isotherm]. Now, the scheme in the model discussed in Sec. V B runs in the opposite direction:  $S(\omega)$  is imposed and  $t(\omega)$  is sought. Substituting  $\dot{S} = \dot{\omega}(dS/d\omega)$  into Eq. (5.8) and solving for  $t$  by separation of variables, we obtain the following expression for the total time  $t$  it takes the engine to pass from  $\omega_i$  to  $\omega_f$  along a given polarization path  $S(\omega)$ :

$$t = -\frac{1}{a} \int_{\omega_i}^{\omega_f} \frac{(dS/d\omega)d\omega}{e^{q\beta\omega} [2(1 + e^{\beta\omega})S + e^{\beta\omega} - 1]}. \quad (5.9)$$

The semigroup heat transfer law is obtained from  $\dot{Q} = \omega\dot{S}$  [eq. (2.4b)] by substituting Eq. (5.8) into it. We let  $\beta'$  be the current temperature of the working fluid so that

$$S = -\frac{1}{2} \tanh(\beta'\omega/2).$$

This results in

$$\dot{Q} = \omega\dot{S} = a\omega e^{q\beta\omega} \frac{(e^{\beta'\omega/2} - e^{(\beta - \beta'/2)\omega})}{\cosh(\beta'\omega/2)}, \quad (5.10)$$

which is very different from any of the phenomenological laws treated in the past. This is because Eq. (5.10) is by no means limited to the vicinity of equilibrium. Expanding  $\dot{Q}$  in  $\beta'$  around  $\beta' = \beta$  to the first order in  $(\beta' - \beta)$  yields the corresponding linear law of irreversible thermodynamics which applies near equilibrium:

$$\dot{Q} \approx \frac{a\omega^2 e^{(q+1/2)\beta\omega}}{\cosh(\beta\omega/2)} (\beta' - \beta). \quad (5.11)$$

The explicit expression for the heat transfer coefficient,

$$L = a\omega^2 e^{(q+1/2)\beta\omega} / \cosh(\beta\omega/2),$$

reveals that even near equilibrium  $L$  is not at all constant. Rather, it depends upon  $\beta$  and  $\omega$ , which means that  $L$  is also time dependent.  $L$  can be taken as approximately constant only if it does not change much within the allowed region of  $\beta$  and  $\omega$ . Thus, we see that phenomenological heat transfer laws might be sufficient from a practical point of view, but are very restrictive from a more general point of view.

## B. The engine of the Curzon–Ahlborn type

### 1. The cycle

The cycle of the Curzon–Ahlborn type is characterized in the following way: while thermally coupled to the heat bath of constant temperature  $\beta_h$ , the working fluid's temperature is also constant and equals  $\beta'_h$ ; and while thermally coupled to the cold bath of constant temperature  $\beta_c$ , the working fluid's temperature is also constant and equals  $\beta'_c$ . These two irreversible isotherms are connected by two adiabats:  $S = S_1$  and  $S = S_2$  ( $S_1 < S_2$ ). Cycle  $1' \rightarrow 2' \rightarrow 3' \rightarrow 4' \rightarrow 1'$  in Fig. 5 is of the Curzon–Ahlborn type, while cycle  $1 \rightarrow 2 \rightarrow 3 \rightarrow 4 \rightarrow 1$  in the same figure is the reversible cycle operated with the same values of  $\beta_h, \beta_c, S_1$ , and  $S_2$ . The efficiency of the cycle of the Curzon–Ahlborn type is  $1 - \beta'_c/\beta'_h$ . If the engine is to generate positive power  $\beta_c > \beta'_c > \beta'_h > \beta_h$  must hold. For  $\beta_c = \beta'_c > \beta'_h = \beta_h$  the reversible cycle is obtained and therefore maximum efficiency and zero power. For  $\beta'_c = \beta'_h$  we have a short circuit and therefore zero power and zero efficiency. We seek, as we always do in the Curzon–Ahlborn problem, the values of  $\beta'_c$  and  $\beta'_h$  between these two extremes for which the power has a maximum.

### 2. The power

The average power per cycle of the engine,  $P$ , is given by

$$P = -W_{\text{tot}} / (t_c + t_h), \quad (5.12)$$

where  $W_{\text{tot}}$  is the total work per cycle, and  $t_c$  and  $t_h$  are the

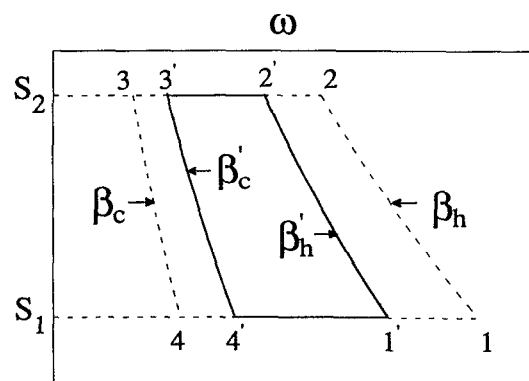


FIG. 5. The cycle  $1' \rightarrow 2' \rightarrow 3' \rightarrow 4' \rightarrow 1'$  is of the Curzon–Ahlborn type.  $\beta'_h$  and  $\beta'_c$  are the temperatures of the working fluid when thermally coupled to the hot ( $\beta_h$ ) and cold ( $\beta_c$ ) baths, respectively. The values of the field at  $1'$ ,  $2'$ ,  $3'$ , and  $4'$  are given by  $\omega'_1 = -2 \tanh^{-1}(2S_1)/\beta'_h$ ,  $\omega'_2 = -2 \tanh^{-1}(2S_2)/\beta'_h$ ,  $\omega'_3 = -2 \tanh^{-1}(2S_2)/\beta'_c$ , and  $\omega'_4 = -2 \tanh^{-1}(2S_1)/\beta'_c$ . The cycle  $1 \rightarrow 2 \rightarrow 3 \rightarrow 4 \rightarrow 1$  is the reversible cycle operating with the same  $\beta_c, \beta_h, S_1$ , and  $S_2$ .

periods of time the working fluid spends along the cold and hot isotherms, respectively. The time spent along the adiabats is negligible since the adiabats are reversible irrespective of  $\omega(t)$  (cf. Sec. II C). —  $W_{\text{tot}}$  is also the work produced by a reversible cycle operating between  $\beta'_h$  and  $\beta'_c$ . It is obtained using Eqs. (2.4a), (2.7), and (2.8):

$$-W_{\text{tot}} = (1/\beta'_h - 1/\beta'_c)F(S_1, S_2), \quad (5.13a)$$

where

$$F(S_1, S_2) = \ln \left\{ \frac{\cosh[\tanh^{-1}(2S_2)]}{\cosh[\tanh^{-1}(2S_1)]} \right\} + 2S_1 \tanh^{-1}(2S_1) - 2S_2 \tanh^{-1}(2S_2) \quad (5.13b)$$

is the total entropy input along the hot branch which is equal to the total entropy output along the cold branch (endoreversibility).  $t_h$  is obtained by substituting  $S(\omega) = -\frac{1}{2} \tanh(\beta'_h \omega/2)$ ,  $\omega_i = \omega'_1$  and  $\omega_f = \omega'_2$  into Eq. (5.9). Changing the integration variable to  $x = \beta'_h \omega$ , we obtain

$$t_h = \frac{1}{2a} \int_{-2 \tanh^{-1}(2S_1)}^{-2 \tanh^{-1}(2S_2)} [e^{q\alpha_h x} (e^{\alpha_h x} - e^x) (1 + e^{-x})]^{-1} dx, \quad (5.14a)$$

where  $\alpha_h = \beta_h/\beta'_h$ .  $t_c$  is obtained in a similar manner by substituting  $S(\omega) = -\frac{1}{2} \tanh(\beta'_c \omega/2)$ ,  $\omega_i = \omega'_3$ , and  $\omega_f = \omega'_4$  into Eq. (5.9) and changing the integration variable to  $x = \beta'_c \omega$ :

$$t_c = \frac{1}{2a} \int_{-2 \tanh^{-1}(2S_2)}^{-2 \tanh^{-1}(2S_1)} [e^{q\alpha_c x} (e^{\alpha_c x} - e^x) (1 + e^{-x})]^{-1} dx, \quad (5.14b)$$

where  $\alpha_c = \beta_c/\beta'_c$ . For simplicity, the same values of  $a$  and  $q$  are assumed for both hot and cold isotherms. Substituting Eqs. (5.13) and (5.14) into Eq. (5.12), we obtain

$$P = \frac{2aF(S_1, S_2) \left( \frac{1}{\beta'_h} - \frac{1}{\beta'_c} \right)}{\int_{-2 \tanh^{-1}(2S_2)}^{-2 \tanh^{-1}(2S_1)} \frac{1}{1 + e^{-x}} \left( \frac{e^{-q\alpha_c x}}{e^{\alpha_c x} - e^x} - \frac{e^{-q\alpha_h x}}{e^{\alpha_h x} - e^x} \right) dx} \quad (5.15)$$

This is the quantity whose maximum as a function of  $\beta'_c$  and  $\beta'_h$  we seek, for given  $\beta_h, \beta_c, S_1$ , and  $S_2$ . We were unable to evaluate the integral in the denominator of Eq. (5.15) (referred to from now on as the “time integral”) in closed form for the general case. The maximization in the general case was therefore carried out numerically and will be presented in Sec. V B 4. A complete analytical solution was found in the high-temperature limit (the “classical” limit) and will be presented in Sec. V B 3. Before we turn to those solutions we would like to draw attention to some of the general properties of the power function in Eq. (5.15).

(1) The factor  $2aF(S_1, S_2)$  is a constant in the optimization scheme pursued. It therefore does not have any effect on the values of  $\beta'_h$  and  $\beta'_c$  at maximum power. Note, however, that those values are still dependent upon the values of  $S_1$  and  $S_2$  since the latter appear in the limits of the time

integral as well.  $a$ , on the other hand, appears in the above-mentioned factor only and does not affect the values of  $\beta'_c$  and  $\beta'_h$  at maximum power at all. The linear dependence of  $P$  upon  $a$  exhibits a self-evident physical trend.

(2)  $t_c$  is a homogeneous function of zeroth order in  $\beta_c$  and  $\beta'_c$  [Eq. (5.14b)], and so is  $t_h$  in  $\beta_h$  and  $\beta'_h$  [Eq. (5.14a)].  $W_{\text{tot}}$  is homogeneous of the first order in  $\beta'_c$  and  $\beta'_h$  [Eq. (5.13)].  $P$  is therefore homogeneous of the first order in  $\beta_c, \beta_h, \beta'_c$ , and  $\beta'_h$ . Maximizing  $P$ , for given  $\beta_c$  and  $\beta_h$ , will therefore provide in a straightforward manner the solution for any other  $\beta_h$  and  $\beta_c$  corresponding to the same  $\beta_h/\beta_c$  ratio. This property allows for the reduction of one degree of freedom ( $\beta_h/\beta_c$  instead of  $\beta_h$  and  $\beta_c$ ). It also implies that the efficiency,  $1 - \beta'_h/\beta'_c$ , and time ratio,  $t_c/t_h$ , depend on the temperatures ratio  $\beta_h/\beta_c$  only and not on the specific values of  $\beta_h$  and  $\beta_c$ .

(3) The integrand of the integrals in Eqs. (5.14) behaves very differently along different regions of the  $x$  axis.

(a) For small  $x$  the integrand’s absolute value rises rapidly as  $x$  decreases. When  $x$  approaches 0 from above the integrand approaches infinity asymptotically like  $1/[2(\alpha - 1)x]$  ( $\alpha$  is  $\alpha_c$  for the cold branch and  $\alpha_h$  for the hot branch). When the engine operates between very small polarizations  $S_1$  and  $S_2$ , the time integral is evaluated in this region. The limit of very small polarizations corresponds to that of very high temperatures. This subregion may therefore be referred to as “classical.” We therefore see that  $P$  is independent of  $q$  in the classical limit (i.e., independent of the specific model of the bath), and that  $S_2 = 0$  will cause the time integral to diverge (one cannot reach the population inversion threshold in finite time via thermal coupling to a non-negative temperature bath). We note that since  $|\tanh^{-1}(2S)|$  assumes large values only when  $S$  is very close to  $-1/2$ , the classical limit can be expected to have a reasonable validity over a large polarization range.

(b) For large  $x$  the integrand’s absolute value decreases moderately as  $x$  increases. When  $x$  goes to infinity, it decays asymptotically to zero like  $e^{-(1 - \alpha_h q)x}$  for the hot branch or  $e^{-\alpha_c(1 - q)x}$  for the cold branch. When the engine operates between very large polarizations ( $S_1, S_2 \rightarrow -1/2$ ), the time integral is evaluated in this region, which corresponds to very low temperatures and may therefore be regarded as “quantum mechanical.” The power clearly depends on  $q$  in this region. Also note that the time integral converges even when  $S_1 = -1/2$ .

(4)  $-W_{\text{tot}}$  converges when  $S_1$  approaches  $-1/2$ :

$$\lim_{S_1 \rightarrow -\frac{1}{2}} (-W_{\text{tot}}) = \left( \frac{1}{\beta'_h} - \frac{1}{\beta'_c} \right) [\ln(2) - 2S_2 \tanh^{-1}(2S_2)] + \ln[\cosh(\tanh^{-1}(2S_2))] \quad (5.16)$$

The time integral also converges in this limit. A cycle with  $S_1 = -1/2$  (and therefore  $\omega'_1 = \omega'_4 = \infty$ ) can therefore be pictured. Such a cycle is constructed out of two isotherms and only one adiabat:  $S = S_2$  (the isotherms meet at  $\omega = \infty$ ). We stress again that the cycle in this limit produces finite power.

### 3. The maximization of power in the high-temperature limit

Substituting  $S(\omega) = -\frac{1}{2} \tanh(\beta'\omega/2)$  into Eq. (5.9), we obtain

$$t = \frac{\beta'}{2a} \int_{\omega_i}^{\omega_f} \frac{d\omega}{e^{(1+q)\beta\omega} + e^{[(1+q)\beta - \beta']\omega} - e^{(\beta' + q\beta)\omega} - e^{q\beta\omega}}. \quad (5.17)$$

Each of the terms in the denominator can be approximated by  $e^x = 1 + x$  for  $\beta\omega, \beta'\omega \ll 1$ , i.e., in the high-temperature limit. We then obtain

$$t = \frac{1}{2a} \int_{\omega_i}^{\omega_f} \frac{d\omega}{2(\alpha - 1)\omega} = \frac{1}{4a(\alpha - 1)} \ln\left(\frac{\omega_f}{\omega_i}\right), \quad (5.18)$$

where  $\alpha = \beta/\beta'$ . The integrand of the time integral in the high-temperature limit is identical to its asymptotic form at very small polarizations (cf. Sec. V B 2), which is consistent since this is the same limit. Substituting the appropriate  $\omega_i$  and  $\omega_f$  into Eq. (5.18) and replacing  $\tanh^{-1}(2S)$  by  $2S$  (since the polarizations are assumed very small), we obtain  $t_c$  and  $t_h$  in closed form in the high-temperature limit:

$$t_c = \frac{\ln(S_1/S_2)}{4a(\alpha_c - 1)}, \quad (5.19a)$$

$$t_h = \frac{\ln(S_2/S_1)}{4a(\alpha_h - 1)}. \quad (5.19b)$$

Note also that in this limit  $t_c$  and  $t_h$  can be written as products of a common polarization term,  $\ln(S_1/S_2)$ , and a temperature term  $1/[4a(\alpha - 1)]$ . This property is unique to the classical limit and implies the independence of the values of  $\beta'_c, \beta'_h$ , and  $t_c/t_h$  at maximum power from  $S_1$  and  $S_2$ . Expanding to the second-order correction,  $e^x = 1 + x + \frac{1}{2}x^2$ , will wash out this property. From Eq. (5.18) one can also obtain the explicit form of  $\omega(t)$ , in the high-temperature limit, that keeps the working fluid's temperature  $\beta'$  constant along the isothermal path:

$$\omega(t) = \omega(0)e^{-4a(1-\alpha)t}. \quad (5.20)$$

Substituting Eqs. (5.19) and (5.13) into Eq. (5.12), we obtain the power in the high-temperature limit in closed form:

$$P = \frac{4aF(S_1, S_2)}{\ln(S_1/S_2)} \frac{(\beta'_c - \beta'_h)(\beta_c - \beta'_c)(\beta_h - \beta'_h)}{(\beta'_c\beta_h - \beta'_h\beta_c)\beta'_c\beta'_h}. \quad (5.21)$$

We maximize  $P$  by a method similar to that used by Chen and Yan.<sup>3(a)</sup> We first express  $P$  as a function of  $\beta'_c$  and  $\eta = 1 - \beta'_h/\beta'_c$ , rather than of  $\beta'_c$  and  $\beta'_h$  as in Eq. (5.21):

$$P = \frac{4aF(S_1, S_2)}{\ln(S_1/S_2)} \frac{\eta(\beta_c - \beta'_c)[\beta_h - \beta'_c(1 - \eta)]}{(1 - \eta)\beta_c'^2[\beta_h - \beta_c(1 - \eta)]}. \quad (5.22)$$

We then solve  $(\partial P/\partial \beta'_c)|_\eta = 0$  to find the value of  $\beta'_c$  that maximizes  $P$  for a given  $\eta$ :

$$\beta'_c = \frac{2\beta_c\beta_h}{\beta_h + (1 - \eta)\beta_c}. \quad (5.23)$$

Substituting Eq. (5.23) into Eq. (5.22), we obtain the maximum power as a function of efficiency:

$$P(\eta) = \frac{aF(S_1, S_2)}{\ln(S_1/S_2)} \eta \left[ \frac{1}{\beta_h} - \frac{1}{\beta_c(1 - \eta)} \right] \\ = \frac{aF(S_1, S_2)}{\ln(S_1/S_2)} \left[ \frac{\eta(\eta_{\text{rev}} - \eta)}{\beta_h(1 - \eta)} \right], \quad (5.24)$$

where  $\eta_{\text{rev}} = 1 - \beta_h/\beta_c$ .

Chen and Yan obtained a very similar expression for Newtonian engines:<sup>3(a)</sup>

$$P(\eta) = \frac{\kappa_h\kappa_c}{[(\kappa_h)^{1/2} + (\kappa_c)^{1/2}]^2} \eta \left[ \frac{1}{\beta_h} - \frac{1}{\beta_c(1 - \eta)} \right], \quad (5.25)$$

where  $\kappa_h$  and  $\kappa_c$  are the Newtonian thermal conductivities along the hot and cold branches, respectively. The efficiency at maximum power is the same for both models since the  $\eta$ -dependent term in the two power functions is identical. It is given by the well-known Curzon-Ahlborn efficiency:

$$\eta_{\text{max}} = 1 - (\beta_h/\beta_c)^{1/2}. \quad (5.26)$$

The values of  $\beta'_h$  and  $\beta'_c$  at maximum power are readily obtained by substituting Eq. (5.26) into Eq. (5.23):

$$\beta'_{c,\text{max}} = \frac{2\beta_c\beta_h(\beta_c)^{1/2}}{\beta_h(\beta_c)^{1/2} + (\beta_h)^{1/2}\beta_c}, \quad (5.27a)$$

$$\beta'_{h,\text{max}} = \frac{2\beta_c\beta_h(\beta_h)^{1/2}}{\beta_h(\beta_c)^{1/2} + (\beta_h)^{1/2}\beta_c}. \quad (5.27b)$$

Substituting Eqs. (5.27) into Eqs. (5.19), the time ratio,  $t_c/t_h$ , and the cycle period,  $t_c + t_h$ , at maximum power, are obtained:

$$\left(\frac{t_c}{t_h}\right)_{\text{max}} = \left(\frac{\beta_h}{\beta_c}\right)^{1/2}, \quad (5.28)$$

$$(t_c + t_h)_{\text{max}} = \frac{\ln(S_1/S_2)}{2a} \left[ \frac{1 + (\beta_h/\beta_c)^{1/2}}{1 - (\beta_h/\beta_c)^{1/2}} \right]. \quad (5.29)$$

The average rate of entropy production,  $-(\beta_h Q_h + \beta_c Q_c)/(t_c + t_h)$ , at maximum power is also readily obtained in this limit from Eqs. (5.29) and (2.4b):

$$\left(\frac{\Delta\sigma_{\text{cycle}}}{t_c + t_h}\right)_{\text{max}} = \frac{2a(S_1^2 - S_2^2)}{\ln(S_1/S_2)} \\ \times [(\beta_c/\beta_h)^{1/2} - (\beta_h/\beta_c)^{1/2}]. \quad (5.30)$$

The effectiveness,  $W_{\text{tot}}/W_{\text{rev}}$ , at maximum power is simply given by

$$\left(\frac{W_{\text{tot}}}{W_{\text{rev}}}\right)_{\text{max}} = \frac{1}{2} \quad (5.31)$$

at this limit ( $W_{\text{rev}}$  is the total work per cycle produced by a reversible engine operating between the same  $S_1, S_2, \beta_c$ , and  $\beta_h$ ). Finally, the maximum power itself is obtained by substituting Eq. (5.26) into Eq. (5.24):

$$P_{\text{max}} = \frac{aF(S_1, S_2)}{\ln(S_1/S_2)} \frac{1}{\beta_h} [1 - (\beta_h/\beta_c)^{1/2}]^2. \quad (5.32)$$

Thus, in the high-temperature limit, the spin-1/2 engine has a power function [Eq. (5.24)] very similar to that of Newtonian engines [Eq. (5.25)]. Its efficiency at maximum

power, at this limit, is therefore the same as that of Newtonian engines, namely the Curzon–Ahlborn efficiency [Eq. (5.26)]. Do these results come about because the semigroup heat transfer law turns into a Newtonian heat transfer law in the high-temperature limit? This is an important question. Indeed, whatever the answer is, a firm relationship had already been established by the results obtained so far between Newtonian engines and the classical limit of the spin-1/2 quantum engine. However, a positive answer will also imply that the validity of our results is just as limited as the validity of the results obtained for Newtonian heat engines. A negative answer, on the other hand, will suggest that the Curzon–Ahlborn efficiency and related quantities are really classical limit figures, whose validity is not necessarily limited to Newtonian engines. In order to find the answer we take the high-temperature limit of  $\dot{Q}$  [Eq. (5.10)] and obtain

$$\dot{Q} = a\omega^2(\beta' - \beta). \quad (5.33)$$

This might appear to be the linear law of irreversible thermodynamics, which is the same as Newton's law at high temperatures, but it is not. This is because  $\omega$  is explicitly time dependent and its time dependence is actually governed by  $\beta'$  [Eq. (5.20)]. Substituting Eq. (5.20) into Eq. (5.33), we obtain

$$\dot{Q} = a\omega^2(0)e^{-8(1-\beta/\beta')t}(\beta' - \beta). \quad (5.34)$$

This reduces to a real linear law only if we add another limit besides the high-temperature limit, namely that of  $\beta'$  very close to  $\beta$ :  $|\beta' - \beta| \ll \beta'$ . These two limits must indeed hold for Newtonian heat conduction to be valid. The answer to the question above is therefore negative. The high-temperature limit, “the classical limit,” is the only limit required for the Curzon–Ahlborn efficiency to hold, at least for the spin-1/2 engine. Proximity to thermal equilibrium, which is explicitly assumed if Newtonian heat conduction is to hold, is not necessary. The Curzon–Ahlborn efficiency is therefore probably more general than its original derivation<sup>2</sup> suggests.

The time ratio in Eq. (5.28) should also be pointed out. It is the same as the number of steps ratio at maximum power found for the step cycle in the same high-temperature limit [Eq. (4.8)]. This is quite surprising since the two cycles are very different from each other and indeed no other quantity associated with maximum power possesses such a similarity. If one looks for a relation characterizing the point of maximum power for a large class of irreversible Carnot-type cycles, the time ratio is clearly a better candidate than the efficiency.

For a Newtonian engine, the time ratio at maximum power was found to be<sup>2</sup>

$$t_c/t_h = \kappa_h/\kappa_c, \quad (5.35)$$

where  $\kappa_h$  and  $\kappa_c$  are the thermal conductivities along the hot and cold branches, respectively. This seems to contradict the suggestion raised in the last paragraph, but it does not. Thermal conductivity has a clear meaning only with relation to Newtonian conduction. The closest expression to thermal conductivity in the semigroup heat transfer law is  $a\beta\beta'\omega^2$  [cf. Eq. (5.33)]. This is not a constant and we therefore average it over the whole branch such that

$$\kappa = \int_{\omega_i}^{\omega_f} a\beta\beta'\omega^2 d\omega / (\omega_f - \omega_i)$$

by definition. We then obtain  $\kappa_h/\kappa_c = (\beta_h\beta'_c)/(\beta_c\beta'_h)$ . At the maximum power point,

$$\frac{\kappa_h}{\kappa_c} = \left(\frac{\beta_h}{\beta_c}\right)^{1/2}. \quad (5.36)$$

We can therefore conclude that by exploring the phenomenological thermal conductivity by means of a less phenomenological theory we get the same time ratio:  $t_c/t_h = (\beta_h/\beta_c)^{1/2}$ , even for Newtonian engines.

#### 4. The maximization of power in the general case, numerical results

The high-temperature limit performance at maximum power depends on the values of  $\beta_c$  and  $\beta_h$  only. The number of free parameters can be further reduced to one, namely  $\beta_h/\beta_c$ , if we utilize the homogeneous property of the power function (cf. Sec. V B 2). Other parameters, besides  $\beta_h/\beta_c$ , appear to affect the performance at maximum power when we go beyond this limit, namely  $S_1$ ,  $S_2$ , and  $q$ .

The optimization problem is solved numerically in the following manner: For given values of  $\beta_h$ ,  $\beta_c$ ,  $S_1$ ,  $S_2$ , and  $q$  the power function [Eq. (5.15)] is evaluated for different values of  $\beta'_h$  and  $\beta'_c$  ( $\beta_h < \beta'_h < \beta'_c < \beta_c$ ), and the values of  $\beta'_h$  and  $\beta'_c$  at maximum power are sorted out. The main numerical effort lies in the evaluation of the time integral [the denominator in Eq. (5.15)], established by open Chebyshev Gaussian quadrature (supplemented by Lagguere Gaussian quadrature for the evaluation of the exponential tail in the asymptotic case:  $S_1 = -1/2$ ).

The results are exhibited in the following manner: For given values of  $q$ ,  $S_2/S_1$ , and  $\beta_h/\beta_c$  we plot the quantity of interest at maximum power vs  $S_1$  ( $0 \geq S_1 \geq -1/2$ ). We plot curves corresponding to different values of  $S_1/S_2$  on the same figure ( $0 < S_2/S_1 < 1$ ), which is equivalent to scanning the allowed region of the  $(S_1, S_2)$  plane. The values for  $S_1 = 0$  correspond to the high-temperature limit (which is the same as the low polarization limit).

We define new relative and renormalized variables that allow for a quick comparison of the performance in the quantum region to the performance in the classical limit. We follow these variables as functions of the above-mentioned parameters. The efficiency and time ratio at maximum power are the most informative quantities and the new variables are defined accordingly by

$$\tilde{\eta} = \left(\frac{\eta - \eta_{cl}}{\eta_{cl}}\right)_{\max}, \quad \tilde{\tau} = \left[\frac{(t_c/t_h) - (t_c/t_h)_{cl}}{(t_c/t_h)_{cl}}\right]_{\max}, \quad (5.37)$$

where “cl” refers to the value of the same quantity at maximum power in the high-temperatures limit, and “max” indicates that the value of the quantity inside the preceding parentheses is given at maximum power.

The effect of  $\beta_h/\beta_c$  is demonstrated in Figs. 6 and 7, where  $\tilde{\eta}$  and  $\tilde{\tau}$ , respectively, are plotted for different values of  $\beta_h/\beta_c$  and for  $q = -0.5$ . The affect of  $q$  is demonstrated in Figs. 8 and 9, where, similarly,  $\tilde{\eta}$  and  $\tilde{\tau}$  are plotted for differ-

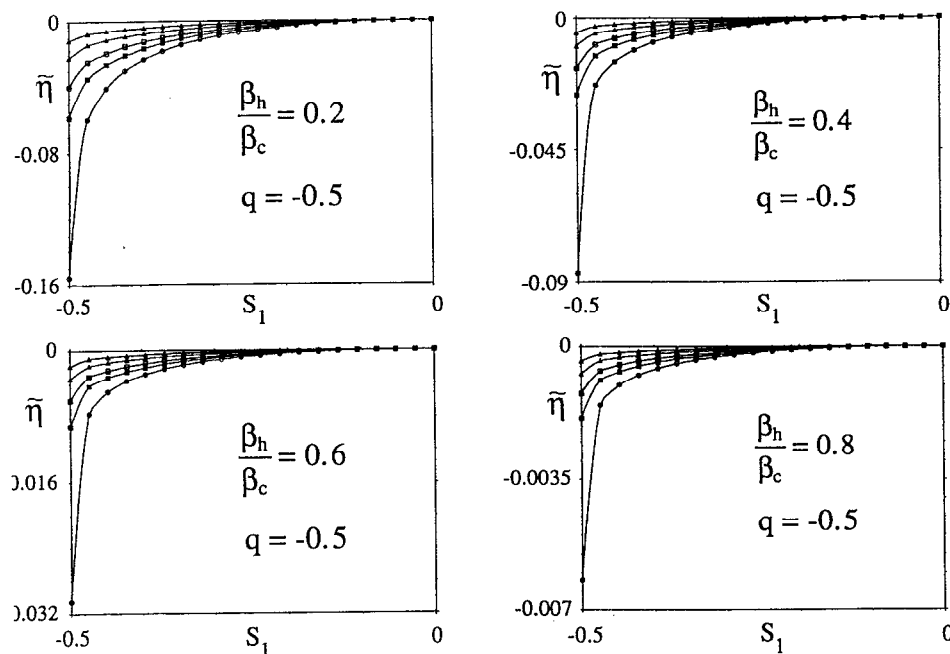


FIG. 6.  $\tilde{\eta}$  as a function of  $S_1$  and  $S_2$  for different values of  $\beta_h/\beta_c$  and  $q = -0.5$ . The different curves in each plot correspond to different values of  $S_1/S_2$  by the following key: ( $\Delta$ ) —  $S_1/S_2 = 0.113$ ; ( $\blacktriangle$ ) —  $S_1/S_2 = 0.350$ ; ( $\square$ ) —  $S_1/S_2 = 0.628$ ; ( $\blacksquare$ ) —  $S_1/S_2 = 0.797$ ; ( $\circ$ ) —  $S_1/S_2 = 0.990$ . Note that the dependence on the temperature ratio essentially amounts to a change in scale.

ent values of  $q$  and for  $\beta_h/\beta_c = 0.2$ .

The following conclusions can be drawn from the results in Figs. 6–9.

(1) The relative deviations of the values of  $\eta_{\max}$  and  $(t_c/t_h)_{\max}$  from the corresponding values at the classical limit are very minor over most of the polarization range. Very large polarizations are required for a significant difference to appear. This is attributed to the fact that the function  $\tanh^{-1}(x)$  (appearing in the limits of the time integral) assumes large values only when  $x$  is very close to 1 (cf. Sec. V B 2).

(2) The sensitivity of  $\tilde{\eta}$  and  $\tilde{\tau}$  towards an increase in the polarization is lower for higher values of  $\beta_h/\beta_c$ . This is because the maximal value of  $\alpha_c$  decreases as  $\beta_h/\beta_c$  increases ( $1 < \alpha_c < \beta_c/\beta_h$ ), which results in relatively small exponents in the time integral. The classical approximation is therefore more valid for higher polarizations, and the deviations from the classical limit are therefore smaller.

(3) Both  $\tilde{\eta}$  and  $\tilde{\tau}$  depend heavily on  $q$ , i.e., on the specific-heat bath. This is qualitatively different from the classical limit maximum power performance, upon which  $q$  did not have any affect (cf. Sec. V B 3). The dependence on  $q$  mani-

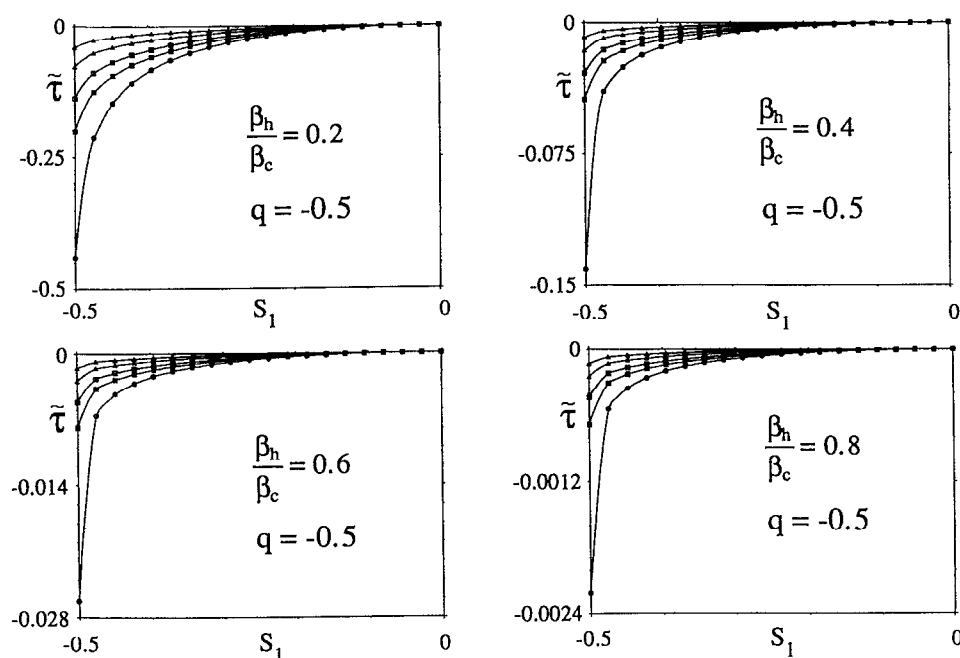


FIG. 7.  $\tilde{\tau}$  as a function of  $S_1$  and  $S_2$  for different values of  $\beta_h/\beta_c$  and  $q = -0.5$ . The different curves in each plot correspond to different values of  $S_1/S_2$  by the following key: ( $\Delta$ ) —  $S_1/S_2 = 0.113$ ; ( $\blacktriangle$ ) —  $S_1/S_2 = 0.350$ ; ( $\square$ ) —  $S_1/S_2 = 0.628$ ; ( $\blacksquare$ ) —  $S_1/S_2 = 0.797$ ; ( $\circ$ ) —  $S_1/S_2 = 0.990$ . Note that the dependence on the temperature ratio essentially amounts to a change in scale.

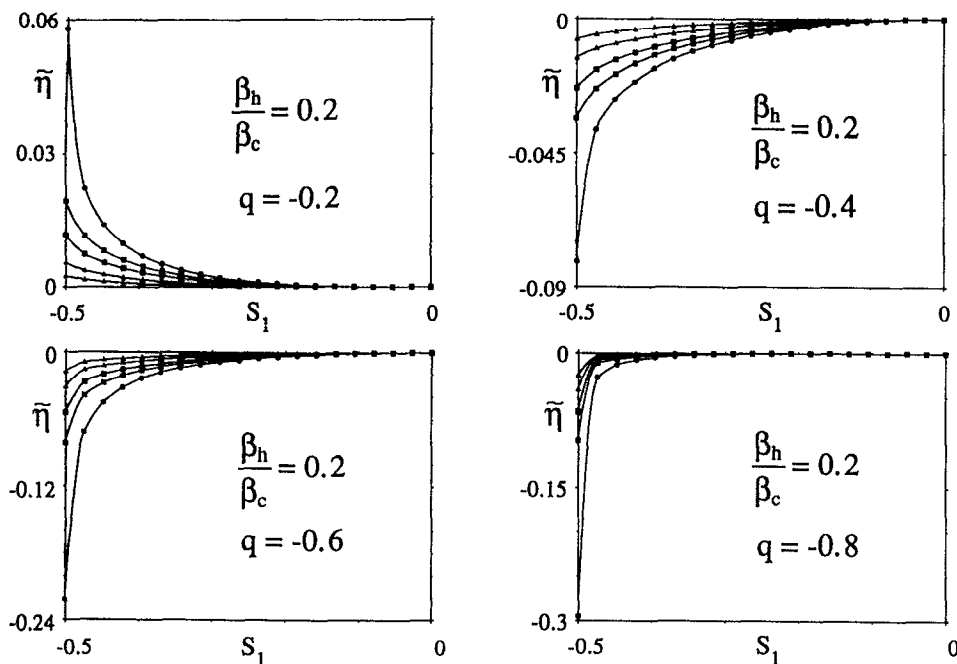


FIG. 8.  $\tilde{\eta}$  as a function of  $S_1$  and  $S_2$  for different values of  $q$  and  $\beta_h/\beta_c = 0.2$ . The different curves in each plot correspond to different values of  $S_1/S_2$  by the following key: ( $\Delta$ ) —  $S_1/S_2 = 0.113$ ; ( $\blacktriangle$ ) —  $S_1/S_2 = 0.350$ ; ( $\square$ ) —  $S_1/S_2 = 0.628$ ; ( $\blacksquare$ ) —  $S_1/S_2 = 0.797$ ; ( $\circ$ ) —  $S_1/S_2 = 0.990$ .

feats itself most astonishingly by a change of sign of  $\tilde{\eta}$  (between  $q = -0.2$  and  $q = -0.3$  for  $\beta_h/\beta_c = 0.2$ ) and  $\tilde{\tau}$  (around  $q = -0.6$  for  $\beta_h/\beta_c = 0.2$ ). The transition involves a gradual inversion in order of the different curves, corresponding to different values of  $S_1/S_2$ , such that the lowest curve becomes the highest and *vice versa*. This must involve curve crossing. The actual behavior in the transition zone turns out to involve a temporal loss of the monotonicity characterizing the curves before and after the transition takes place.

The origin of this surprising  $q$  dependence is exposed when we compare the integrand in Eqs. (5.14) for different

values of  $q$ , with its classical limit which is independent of  $q$  [Eq. (5.18)]. The absolute value of the integrand will be simply referred to as “the integrand” in what follows. For  $q \rightarrow -1$  the integrand approaches the classical limit from *above* as  $x$  decreases. For  $q \rightarrow 0$  the integrand approaches the classical limit from *below* as  $x$  decreases. Changing  $q$  from  $-1$  to  $0$  must therefore involve a transition from one type of behavior to the other.

The space under the curve is a measure of the time spent along the isothermal path [Eq. (5.14)]. This time become longer as  $q$  decreases since, as has already been seen, the heat exchange slows down as  $q$  becomes more negative [Eq.

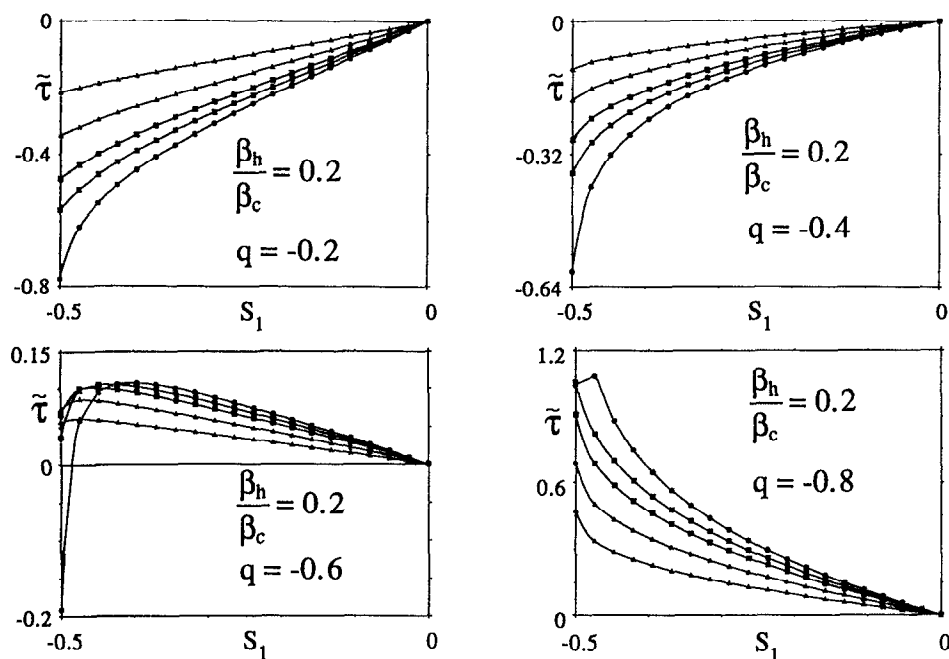


FIG. 9.  $\tilde{\tau}$  as a function of  $S_1$  and  $S_2$  for different values of  $q$  and  $\beta_h/\beta_c = 0.2$ . The different curves in each plot correspond to different values of  $S_1/S_2$  by the following key: ( $\Delta$ ) —  $S_1/S_2 = 0.113$ ; ( $\blacktriangle$ ) —  $S_1/S_2 = 0.350$ ; ( $\square$ ) —  $S_1/S_2 = 0.628$ ; ( $\blacksquare$ ) —  $S_1/S_2 = 0.797$ ; ( $\circ$ ) —  $S_1/S_2 = 0.990$ .

(5.10)]. The classical heat flow may therefore be faster or slower than the heat flow in the quantum region, depending on the value of  $q$ . The efficiency and time ratio at maximum power are measured relative to their values in the classical limit. The sign shift in Figs. 8 and 9 is accounted for by the shift in the rate of heat flow relative to the classical limit which is associated with the change of  $q$ .

Now, we can also understand why  $\eta_{\max}$  decreases as  $q$  changes from 0 to  $-1$  (Fig. 8). The heat exchange slows down as  $q$  become more negative. Less heat is pumped into the engine for a given temperature difference. Increasing the temperature difference increases the amount of heat pumped in and reduces the efficiency. The net effect is probably that of increasing power. Maximum power is therefore obtained at lower efficiencies.

A remark concerning the parameters  $q$  and  $a$  is in order. The parametrization of the bath in terms of  $q$  and  $a$  chosen here is the simplest possible. The physical meaning of  $q$  and  $a$  remains obscure to a large extent. Explicit expressions for  $\gamma_+$  and  $\gamma_-$  can be obtained in the weak-coupling limit in terms of correlation functions of the bath.<sup>6(b)</sup> To this end one must solve for the dynamics of the bath. This can be accomplished analytically for two bath types, namely the harmonic bath (e.g., a radiation field) and the Ising bath (e.g., the Heisenberg ferromagnet).<sup>6(b)</sup> In the former  $a$  turns out to be proportional to  $\omega^3$  on account of the mode density in three dimensions (3D). The assumption of constant  $a$  is therefore not valid unless a 1D bath is discussed.  $q$  approaches  $-1$  for  $\beta\omega \gtrsim 2$  in this case, and is meaningless for high temperatures (where it is eliminated from the equations anyway). The main physical conclusion that the performance is affected by the nature of the bath seems to be independent of the parametrization used. A better understanding of this phenomenon will be achieved by analyzing systems with specific bath models of the two types mentioned above.

(4) The classical equality:  $(t_c/t_h) = 1 - \eta_{\max}$  [cf. Eqs. (5.26) and (5.28)], no longer holds in the general case, since  $\bar{\tau}$  and  $\bar{\eta}$  respond very differently to an increase in the polarization. Qualitatively, this results from the different and much more complex dependence of the time integral on  $\beta'_h$  and  $\beta'_c$  in the general case [Eq. (5.15)] compared with the classical limit [Eq. (5.19)].

## VI. SUMMARY

In the Introduction, three general questions were presented as motivating this research. We conclude by examining the extent to which the spin-1/2 model engine provided us with answers to these questions.

I. All the results of the Curzon–Ahlborn analysis can be fully reproduced for the spin-1/2 engine in the classical limit (cf. Sec. V B 3). Proximity to thermal equilibrium, implicitly implied by the use of Newtonian heat conduction in the original derivation, is not required. Furthermore, by replacing the Newtonian conduction with the less phenomenological semigroup relaxation law, new relations appear, such as the time ratio in Eq. (5.28). All these conclusions remain valid when the spin-1/2 fluid is replaced by a fluid containing many noninteracting harmonic oscillators.<sup>12</sup> The fact

that these two systems differ in many respects<sup>13</sup> does not seem to make a difference in the classical limit. It is very tempting to propose that this result can be generalized to all fluids of the “ideal-gas” type (i.e., containing noninteracting systems).

II. Typical results of finite-time thermodynamics, such as Eqs. (4.8) and (5.26), are obtained for quantum-mechanical engines in the classical limit. Going beyond this limit makes both a qualitative and a quantitative difference. Quantitatively, the numerical values of the operation parameters at maximum power are not given by the classical expressions. Qualitatively, the details of the model, which were blurred by the classical limit, now make a difference:  $(N_c/N_h)_{\max}$  will not be the same for two step cycles, one with spin-1/2 systems and the other with particles in a box as the working fluid;  $\eta_{\max}$  and  $(t_c/t_h)_{\max}$  depend on the specific-heat bath, etc. This signals the great diversity and complexity of the field of far-from-equilibrium quantum-mechanical finite-time thermodynamics. The approach of the quantum-mechanical engine towards the classical limit received quantitative consideration only for the spin-1/2 engine of the Curzon–Ahlborn type (cf. Sec. V B 4). The classical approximation was found to apply reasonably well for most of the polarization range. Replacing the spin-1/2 systems with harmonic oscillators results in a time integral of a slightly different form [the term  $(1 + e^{-x})$  in Eqs. (5.14) is replaced by  $(1 - e^{-x})$ ].<sup>12</sup> The behavior beyond the classical limit is therefore different but the two models converge again in the opposite limit of low temperature. The interpretation is straightforward: most of the population lies in the first two levels at low temperatures and the oscillator may be regarded as a two-level system. The classical approximation also applies reasonably well for most of the oscillator population range.

III. The discrete nature of the working fluid’s energy (where the quantum-mechanical nature of the engine lies, cf. Sec. II C) mostly affects the isotherms in the region of large polarization. The impact upon the power function lies in the time integral. The latter originated from a quantum-mechanical equation of motion for which the discrete nature of energy is already built in. We discussed the operation at large polarizations in Sec. V B 4. The deviations from the classical limit, demonstrated there, are therefore the direct consequence of the discrete nature of energy, i.e., of quantum mechanics *per se*.

Encouraged by the results of the present study, we intend to pursue the line of research initiated here. The model discussed above may be expanded in many directions, a few of which are listed below.

1. The working fluid may consist of other simple quantum-mechanical systems. Harmonic oscillators and other spin systems may serve as examples. Systems having three or more energy levels may be operated as lasers, so that connections with the results in Ref. 5 may be established. A comparison between systems differing with respect to the dimension of the Hilbert space, the response to changes in the external field, etc. (e.g., spin systems vs harmonic oscillators) is also of interest.

2. Objective functions other than power and constraints dif-

ferent from those discussed above may be used. We have already started studying the performance of the spin-1/2 engine when operated so as to minimize the entropy production. The more difficult task of finding the optimal path by the methods of optimal control theory is also of interest.

3. The magnetic field may rotate. This should impose new quantum-mechanical effects originating from the noncommutability of the observables and is important for engines driven by a radiation field.

4. The specific nature of the bath has a pronounced effect in the quantum-mechanical region. It seems that in order to understand it better more specific models for the baths, containing more physical essence, should be used. The effect of allowing baths with negative temperatures should also be studied.

5. Internal interactions within the working fluid may be included. For example, in the case of the spin-1/2 engine discussed above this can be accomplished by an Ising model.

## ACKNOWLEDGMENTS

The Fritz Haber Research Center is supported by the Minerva Gesellschaft für die Forschung, Munich, Federal Republic of Germany. We thank the participants of the Danish-Israeli workshop on irreversible thermodynamics (29 April–2 May 1991), Professor R. S. Berry, and Professor G. Lindblad for helpful comments and discussions.

<sup>1</sup> For a survey of the field's present state, see *Finite Time Thermodynamics and Thermoconomics*, Vol. 4 in *Advances in Thermodynamics*, edited by S. Sieniutycz and P. Salamon (Taylor & Francis, London, 1991), and references therein.

<sup>2</sup> F. L. Curzon and B. Ahlborn, *Am. J. Phys.* **43**, 22 (1975).

<sup>3</sup> (a) L. Chen and Z. Yan, *J. Chem. Phys.* **90**, 3740 (1989); (b) J. M. Gordon, *Am. J. Phys.* **58**, 370 (1990).

<sup>4</sup> P. Salamon, A. Nitzan, B. Andresen, and R. S. Berry, *Phys. Rev. A* **21**, 2115 (1980).

<sup>5</sup> R. Kosloff, *J. Chem. Phys.* **80**, 1625 (1984).

<sup>6</sup> (a) G. Lindblad, *Commun. Math. Phys.* **48**, 119 (1976); (b) R. Alicki and K. Lendi, *Quantum Dynamical Semigroups and Applications* (Springer-Verlag, Berlin, 1987).

<sup>7</sup> C. Cohen-Tannoudji, B. Diu, and F. Laloe, *Quantum Mechanics* (Wiley, New York, 1977), Vol. 1, Chap. IV.

<sup>8</sup> (a) H. Sphon and J. L. Lebowitz, *Adv. Chem. Phys.* **38**, 109 (1979); (b) R. Alicki, *J. Phys. A* **12**, L103 (1979).

<sup>9</sup> (a) H. B. Callen, *Thermodynamics* (Wiley, New York, 1960), Appendix F; (b) J. A. Fay, *Molecular Thermodynamics* (Addison-Wesley, Reading, MA, 1965), p. 353.

<sup>10</sup> B. Andresen, R. S. Berry, A. Nitzan, and P. Salamon, *Phys. Rev. A* **15**, 2086 (1977).

<sup>11</sup> See, for example: R. Kosloff, *Physica* **110A**, 346 (1982); R. Kubo, M. Toda, and N. Hashitsume, *Statistical Physics II, Nonequilibrium Statistical Mechanics* (Springer-Verlag, Berlin, 1983).

<sup>12</sup> E. Geva and R. Kosloff (unpublished).

<sup>13</sup> The harmonic oscillator and the spin-1/2 system represents two types of systems differing in the following respects: (a) The Hamiltonian of the harmonic oscillator is not bounded while that of the spin-1/2 is. (b) The creation and annihilation operators of the harmonic oscillator are of the Boson type while those of the spin-1/2 are of the Fermion type. See, e.g., W. H. Louisell, *Quantum Statistical Properties of Radiation* (Wiley, New York, 1990), p. 98.